NANO LETTERS

Letter

pubs.acs.org/NanoLett

Large-Scale Spinning of Silver Nanofibers as Flexible and Reliable Conductors

Ya Huang,[†] Xiaopeng Bai,[†] Ming Zhou,[‡] Suiyang Liao,[†] Zongfu Yu,[‡] Yaping Wang,[§] and Hui Wu*[,†]

[†]State Key Laboratory of New Ceramics and Fine Processing, School of Materials Science and Engineering, Tsinghua University, Beijing 100084, China

[‡]Department of Electrical and Computer Engineering, University of Wisconsin, Madison, Wisconsin 53706, United States

[§]Suzhou InReal Optoelectronics Material Technology Co., Suzhou 215000, China

Supporting Information

ABSTRACT: Conducting metal nanowires can be assembled into thin films for flexible electronics and optoelectronics applications including transparent electrodes, nanocircuits, and electronic skin, however, the junction resistances and low aspect ratios still limit its performance. Herein we report high-quality silver nanofibers (AgNFs) synthesized by a gas-assistant solution spinning method. Compared with traditional Ag nanowires that usually have lengths below 100 μm, AgNFs are infinitely long and can be easily assembled into large-scale 2D and 3D flexible conductors with fused junctions between nanofibers. The AgNF networks showed high transparency, low sheet resistance (e. g, 6 Ω sq^{-1} at ∼97% transparency), and high flexibility as transparent electrodes, whereas the 3D AgNF sponge could be used as a deformable and robust 3D conductor.

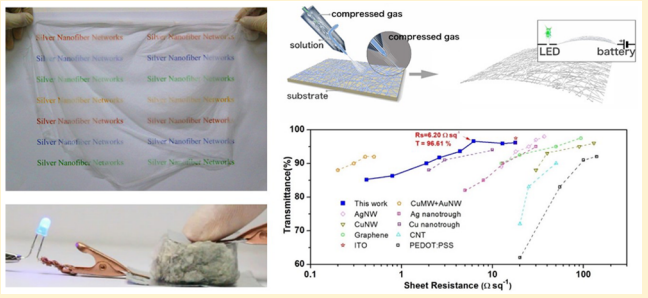

KEYWORDS: *Ag nanofibers, transparent electrode, blow spinning, flexible electronics, 3D conductor*

Silver has the highest electrical conductivity among metals, as well as high thermal conductivity; thus, it is widely used as a conductive filler, connector, and adhesive for electronic devices.[1,2] In recent years, Ag nanowires (AgNWs), which typically have a diameter of 100−500 nm and length of 10−100 μm, have been developed as fundamental building blocks for many important electronic and optoelectronic applications, such as transparent electrodes, wearable electronics, and sensors.[3−5] One famous example is the successful application of AgNWs as transparent electrodes to replace indium tin oxide (ITO).[6,7] Transparent electrodes are widely used in optoelectronics, such as displays, solar cells, smart windows, touch screens, and light-emitting diodes (LED).[8] ITO is recognized as the most common transparent electrode material but suffers from some crucial drawbacks, such as high cost, scarcity of indium, damage of organic substrates during high-temperature sputtering, and most importantly lack of flexibility.[6,9] These problems have motivated research on novel transparent conductors. Random or aligned networks of AgNWs represent a promising class of transparent conductive materials to replace ITO. AgNWs can form two-dimensional (2D) random networks on supporting substrates, such as glass and polymer,[4,10,11] with highly conductive percolation pathways to serve as conductive electrodes.[12] AgNWs have excellent mechanical flexibility associated with their small lateral diameters, so the transparent conductive networks of AgNWs are highly electromechanically robust and superior to the more fragile ITO film. In general, the performance of AgNW network is limited by wire-to-wire junctions.[7,11,13] Various methods have been used to improve the performance of AgNW networks, including increasing the nanowire length to increase transport distance,[14] decreasing the diameter to reduce light scattering, and annealing of the nanowire junction to reduce resistance.[7,13,15,16] The combination of AgNWs with a second material is also an efficient method to improve performance.[17,18] The performance can also be improved by the application of natural scaffoldings perfected by evolution.[19] Nevertheless, the functionalities of a flexible conductive electrode and the extension of its practical applications significantly rely on the design of AgNW networks and the fast facile fabrication of highly conductive flexible electrodes. Their design and fabrication have also been the focus of recent research in flexible electronics.[8]

Compared with thin film electrodes, three-dimensional (3D) conductors have attracted increasing attention in recent years and feature both high conductivity and large deformation stability; such features enable a wide variety of new applications in wearable displays, electronic skins, and biological actuators.[20−22] One key challenge to achieve high-performance 3D and flexible electronics is fabricating high-performance conductive interconnects, contacts, and electrodes that possess

Received: June 28, 2016
Revised: July 29, 2016
Published: August 22, 2016

DOI: 10.1021/acs.nanolett.6b02654
Nano Lett. 2016, 16, 5846−5851

a remarkable ability to deform with stable conductivity.[23] Recently, a 3D stretchable and compressible metal sponge was fabricated using polymer-assisted metal deposition.[23] The 3D printing of a conductive complex structure with silver nanoparticles can also fabricate a 3D conductor.[24] However, the demonstration process is complicated for most practical applications. Metal is still the first choice of material when considering high conductivity, stability, and low cost. Although bulk metals are normally considered rigid materials, they are very flexible when sufficiently thin and are stretchable when structured into proper shapes.[25] The development of a simple low-cost scalable method to fabricate a highly conductive 3D flexible structure is advantageous.[26−28]

Template-directed synthesis provides the most straightforward means to guide the growth of silver nanocrystals into nanowires.[7] Although AgNWs and nanowires made of other metals can be synthesized with the assistance of templates, the quality of the resulting nanowires usually needs to be improved in terms of crystallinity, surface smoothness, and mass production.[29] Electrospinning has become well-known as a highly effective technique to prepare nanofibers,[30,31] and silver-based conductive nanofibers have been synthesized using this novel electrospinning technique.[31] The present paper reports a gas-assistant solution spinning method for the large-scale synthesis of high-quality continuous Ag nanofibers (AgNFs) and fabrication of 2D and 3D flexible conductors.[32] The grains of crystalline silver are compact, and the length of single AgNFs is larger than 2 mm with a diameter approaching 200 nm. Given that the obtained AgNFs have thin diameters and a high aspect ratio, percolation pathways can be easily formed even with a very low load percentage of AgNFs; these pathways lead to the significant reduction of silver loading compared with the use of AgNWs.[29] AgNFs exhibit excellent flexibility and can withstand mechanical crushing without an obvious increase in resistance. The combination of ultralong AgNFs and fused junctions guarantee good conductivity of the electrodes at a given transmittance. In addition, a new kind of ultralight 3D conductor called silver sponge with remarkable flexibility, compressibility, and stretchability was obtained because of the high-performance conductive interconnects. This silver sponge has a wide range of applications in 3D flexible electronics, such as electronic skin and 3D Joule heater.[33]

The fabrication of our AgNF is based on the blow spinning method in which pressurized airflow is used to stabilize "taylor cone", as shown in Figure 1a. The AgNFs were synthesized by reduction from $AgNO_3$-doped polyvinylpyrrolidone (PVP) composite nanofibers through calcination. The precursor of PVP/$AgNO_3$ fibers were obtained by the blow spinning method in which the spinnability solution was stretched by air flow and evaporated quickly under the action of air flow. Blow spinning is an easy way to fabricate nanofibers and has the same advantages as electrospinning. In the process of blow spinning, the solution solidified into fibers (Figure 1b) by shearing strength produced by compressed air from the nozzle and could be collected on various substrates with different shapes. It is used at room temperature and does not need high voltage and an electric collector for the rapid production of highly conductive AgNFs on nonconductive substrates. High viscosity solution is feasible to fabricate nanofibers because of strong airflow. The blow spinning method can be readily scaled up to fabricate samples with sizes larger than 40 cm in ambient conditions (Figure 1b).

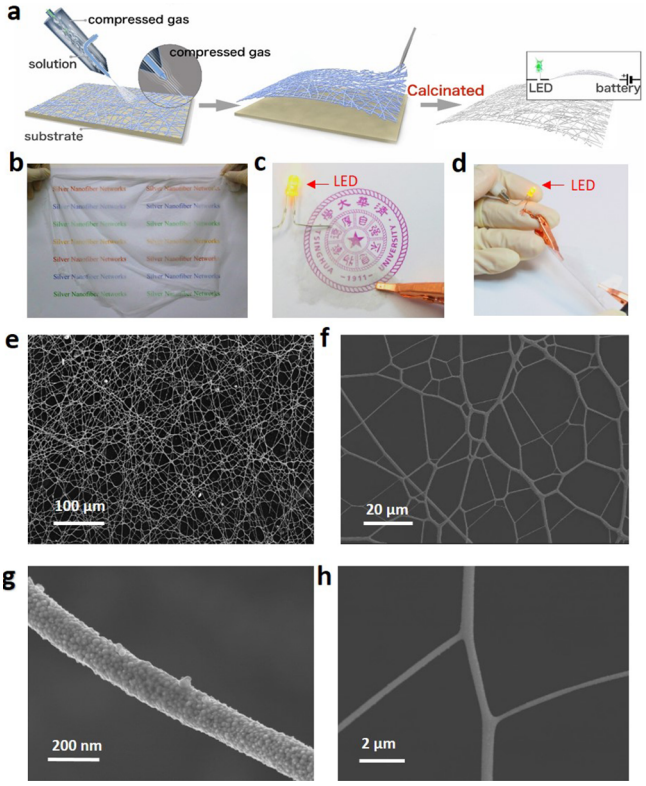

Figure 1. Fabrication and morphology of silver nanofiber network. (a) Schematic of the synthesis of AgNFs. Precursor fibers were first made by blow spinning and then calcined at 280 °C for 2 h. (b) Photograph of precursor PVP/$AgNO_3$ fiber without calcination which shows fabrication of large scale nanofiber network is feasible. (c) Free standing and folded AgNF network is conductive. We connected it in an electric circuit in which an LED is lit. (d) AgNF network attached on a folded PET and is still conductive. SEM images of the top view of the AgNF network at low (e) and high (f) magnifications. (g) SEM image of single AgNF. The silver crystalline grains compact with each other firmly and result in the high conductivity of single silver fibers. (h) The junction of AgNFs. Junctions between different AgNFs weld after calcination. These welded junctions remove the obstruction of electron transportation and guarantee the conductivity of the network.

In calcination, the polymer is oxidized by air and $AgNO_3$ is reduced to silver elementary crystal at a high temperature. $AgNO_3$ is reduced even at room temperature because of its highly active chemical character. Subsequently, PVP/$AgNO_3$ fibers were calcined at 280 °C for 2 h to lose carbon and hydrogen and obtain silver fibers. The optimum temperature of calcination was determined by thermogravimetric analysis (Figure S1) and Raman spectrum (Figure S2). Two Raman active modes at 1352 and 1560 cm^{-1} corresponded to amorphous carbon after the fiber was calcined. Energy dispersive spectroscopy of silver elements (Figure S3) proved that the distribution of silver in the fiber was uniform. The AgNF network is conductive, free-standing, and foldable, as shown in Figure 1c. It can also maintain conductivity after being attached to a variety of soft substrates, such as glass, polyethylene terephthalate (PET) film, and paper (Figure S4), without any surface treatment, so the whole surface is highly conductive. Figure 1e shows a typical example of a AgNF network at a scale bar of 100 μm. Figure 1f presents the top view of the obtained silver fiber network at a large scale bar assembled by 200−1000 nm silver fibers; the minimum diameter approaches 200 nm, and the maximum diameter is

DOI: 10.1021/acs.nanolett.6b02654
Nano Lett. 2016, 16, 5846−5851

about 1 μm. The silver crystalline grains compact with each other firmly, as shown in Figure 1g; this compactness results in the high conductivity of single silver fibers. Silver fibers were also characterized by X-ray diffraction to investigate their crystal structure, as shown in Figure S5. The silver fibers correspond to the normal silver crystal phase, and the grain size of synthesized AgNFs is less than 23 nm from the full width at half-maximum of silver peak at 77.5° of 2θ. As shown in the transmission electron microscope (TEM) image of a single silver fiber in Figure S6, the fiber is combined with compacted silver grains, and the silver grain displays clear lattice fringes, which correspond to the interplanar spacing d = 0.235 nm. On the surface of silver fibers with insufficient calcination, amorphous carbon films are present and have a thickness smaller than 5 nm.

For a nanowire film to be electrically conductive, all its nanowires must be in contact. According to percolation theory, the percolation threshold can be dramatically decreased with the increase in fiber length, as shown in the following equation:

$$l\sqrt{\pi N_c} = 4.236$$

Long nanowires must be used to achieve a conducting path at a low nanowire density. To maximize L/D, that is, the aspect ratio of nanowires, the number of connections between nanowires at a low area fraction must also be maximized.[5] Figure S7 illustrates the microscope photograph of the AgNF network. The length of the obtained AgNF was larger than 2 mm, which resulted in an L/D approaching to 10 000. Most AgNWs synthesized by chemical reaction are shorter than 100 μm.

The conducting AgNF networks combined AgNFs with different scales, including AgNFs with diameters of 200 nm and silver microfibers with diameters approaching 1 μm. The combination of metal microfibers and nanofibers leads to better conductivity of electrodes at a given transmittance than electrodes using single-scale metal wires.[4] Micro- and nanoscale folds of exceptional properties occur naturally in many biological systems, such as leaf veins and spider webs.[15] The diameter of the obtained silver fiber was distributed, and the network was composed of silver fibers with different diameters similar to a leaf vein; this characteristic was beneficial for the performance of the conductive network. The mean diameter of silver fibers is controlled by some technological parameters, such as the polymer concentration of the solution and the speed of the air blowing. For the active layers of many devices, the electrical conductivity of the lateral surface is sufficient to transport electrons only locally from several 100 nm to a few micrometers without serious ohmic loss. The conjunction of microscale and nanoscale silver fibers can reduce sheet resistance at a given transmittance. Nanofibers no longer need to transport electrons for a distance of several millimeters because of the combination of nanofibers and microscale silver fibers.

Junctions between different AgNFs weld after calcination. These welded junctions remove the obstruction of electron transportation and guarantee the conductivity of the network. The density distribution of silver fibers is uniform, and individual nanofibers are naturally interconnected at their junctions during calcination, as shown in Figure 1h.

The sheet resistance of the silver fiber network can be altered by varying the thickness and density of AgNFs. The electro-optical properties of the AgNF network are summarized in Figure 2a, which presents the sheet resistance (Rs) versus transmittance at a wavelength of 550 nm. The resistance of the AgNF network with a transmittance approaching 97% was superior at about 6 $\Omega \cdot sq^{-1}$ compared with the other transparent

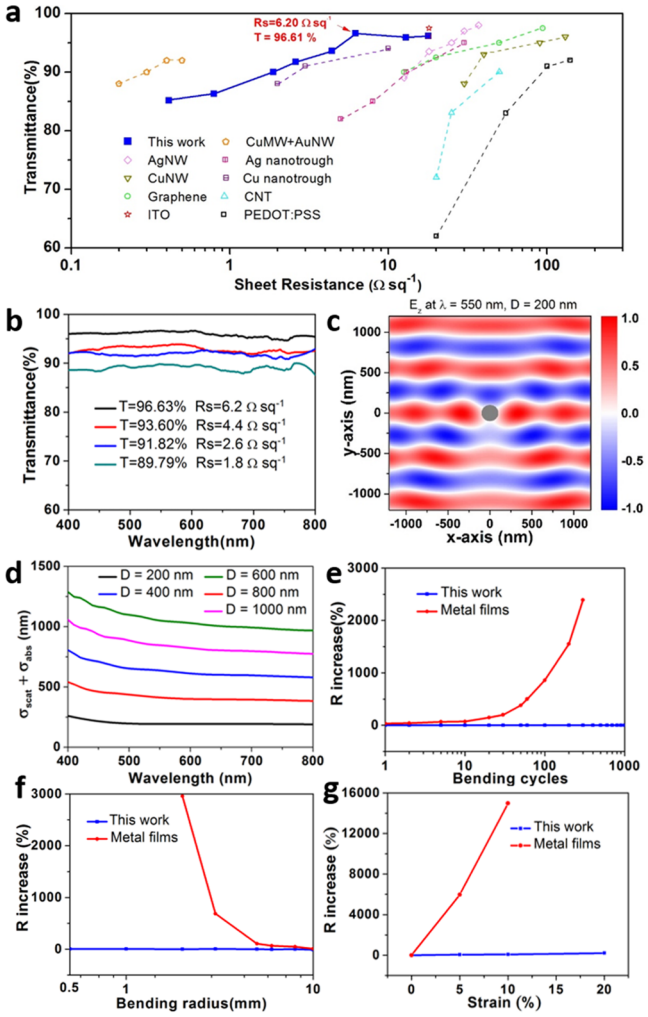

Figure 2. Electrical and optical property measurement. (a) Sheet resistance versus optical transmittance (550 nm) for the AgNF network. The performance of ITO, metal nanowires,[4,35] metal nanotroughs,[34] graphene,[36] CNT,[37] and PEDOT:PSS[4] are shown for comparison. Note that the transmittance mentioned here does not include the transmittance of the substrates. (b) Experimentally measured transmittance spectrum of the AgNF network on glass substrates. High transmission is obtained over the entire visible wavelength range. (c) Simulation of optical scattering by AgNF fiber. The electric field distribution at wavelength of 550 nm. The diameter of the AgNF (gray circle) is 200 nm. Light with z-polarization is normally incident on the AgNF from the top. We used finite element method to solve the Maxwell's equations. Because the AgNF is small, most of the incident light is only disturbed around the AgNF. (d) Simulated cross-section of the AgNFs with different diameters. The results are averaged over two polarizations. The sum of backscattering cross-section σ_{scat} and absorption cross-section σ_{abs} is calculated and plotted. The cross-section does not sensibility depend on wavelength. (e) Sheet resistance versus bending radius for bendable transparent electrodes consisting of AgNF networks or metal films on PET substrates. (f) Variations in resistance of a AgNF electrode and a metal film electrode on PET film as a function of the number of cycles of repeated bending to a radius of 10 mm. (g) Sheet resistance versus uniaxial strain for a stretchable transparent electrode consisting of a AgNF network on PDMS substrate. The rapid degradation of a platinum thin film is shown.

DOI: 10.1021/acs.nanolett.6b02654
Nano Lett. 2016, 16, 5846−5851

conducting electrodes reported in the literature, such as those based on silver nanotrough,[34] solution-processed AgNWs,[4,35] graphene,[36] carbon-nanotube films,[37] and conducting polymers.[4] Sheet resistance is measured by a four-probe method, and the reported resistance of each sample is the average value of several measurements.

The excellent performance of AgNF networks can be well explained by the optical properties of individual AgNFs. We perform full wave simulation to investigate the optical cross sections of AgNFs. Figure 2c shows the electric field distribution when s-polarized light is normally incident on a AgNF from the top. The incident wavelength is 550 nm, and the diameter of the AgNF is 200 nm. The incident light is only slightly disturbed around the AgNF, indicating a small optical cross-section. We further calculated the backscattering cross-section σ_{scat} and absorption cross-section σ_{abs} of AgNFs with different diameters. The cross sections are averaged over s- and p-polarizations. For all AgNFs, the optical cross sections are almost the same as their geometrical cross sections. Therefore, the reflection and absorption of a single layer of AgNF is approximately the same with the filling ratio of AgNFs. As we increase the density of AgNFs, the transmittance decreases as the reflection and absorption increase in Figure 2d, which also agrees well with measurements shown in Figure 2b.

The synthesized AgNFs are mechanically flexible and robust. Deformation was manually made on the network to check the stability and strength of the AgNF network. The network could be crushed and unfolded many times and showed no visible damage (Video S2). After examining the transparent electrode after bending measurements, no obvious degradation in electrical conductivity was found. Unlike metal films, the AgNF network can maintain its mechanical stability after repeated dynamic bending tests. The AgNF network was successfully attached onto aluminum foil and crushed. AgNF was continuous on the crease line, as shown in Figure S8. The mechanical durability of the AgNF network was examined by measuring the change in sheet resistance with bending tests of different radii, as shown in Figure 2f. When the bending radius decreased, the resistance of metal film increased, whereas the resistance of the AgNF network showed nearly no increase. After hundreds of bending processes, the resistance of the network only changed slightly; the metal films would be nearly nonconductive at the same point, as shown in Figure 2e. The stretchability of the AgNF network was examined by transferring the silver fiber networks onto a substrate of polydimethylsiloxane (PDMS) film without surface activation. Sheet resistance increased by 50% after being stretched uniaxially to 5% strain, as shown in Figure 2g.

The continuous silver nanofibers can be further assembled to three-dimensional sponge conductors. The 3D AgNF networks were measured using SEM to further determine the strength of AgNFs. The AgNFs remained continuous during folding. Figure 3a shows the SEM image of the edge of the folded network. Figure 3b shows that the fibers could be folded without fracture. The AgNF did not break when it was bent to 150°. The structure of the AgNF network presented an orientation pattern when it was stretched with uniaxial strain, as shown in Figure 3c. The AgNF network was successfully attached onto flat substrates and a nonplanar surface; it still conducted after crushing and unfolding, as shown in Figure 3d. AgNF electrodes clearly have many advantages, including high transparency, superior flexibility, and ease of transfer. Networks using these electrodes are readily applicable in practical

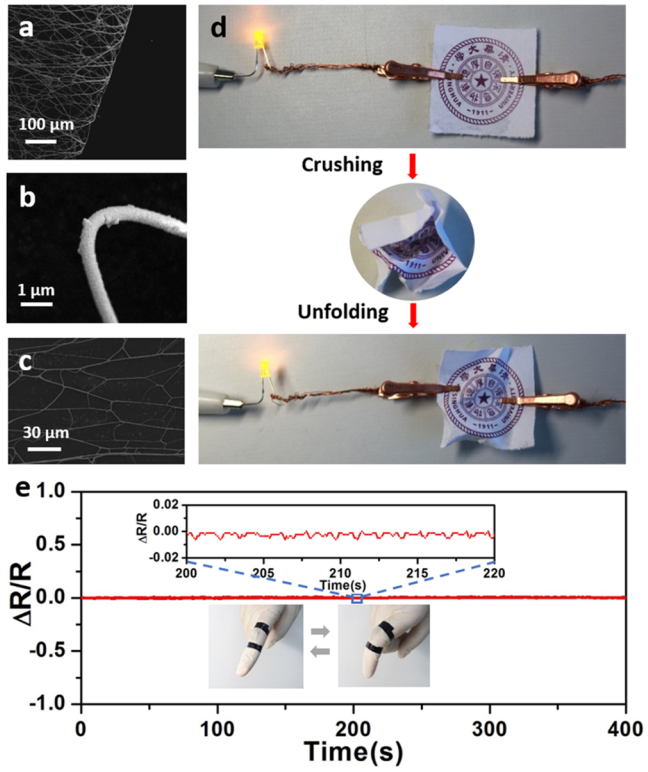

Figure 3. Application of bendable AgNF network. SEM images of the AgNF network after folding at low (a) and high (b) magnifications. (c) SEM image of the AgNF network after stretch. (d) Photographs of "conducting paper" fabricated by transferring AgNF networks onto paper. After crushing and unfolding, the paper remained conductive. (e) Sheet resistance versus bending cycles for a stretchable transparent electrode consisting of the AgNF network on gloves. The negligible degradation of the electrode is shown. Sheet resistance changed periodically with the bending radius of the AgNF network. Photographs of bendable electrodes of the AgNF network attached on the finger are shown.

electronic devices, such as electronic skin. Figure 3e shows current representative data collected on bendable electrodes consisting of an AgNF network attached onto a finger joint. Sheet resistance of the electrodes changed periodically when the finger bent and unbent repeatedly. The bendable and stretchable electrodes showed excellent stability after more than 300 cycles of bending treatment for 400s (Figure 3e).

AgNF sponge was fabricated from entanglement networks in Figure 4a. The sponge retained stable conductivity under repeated bending; its compression deformation (Video S1) and resistance changed periodically when it was pressed, as shown in Figure 4b. In compression tests, the AgNF sponge maintained a negligible value of $\Delta R/R_o$ of up to 5% in the whole range of compression strains (Figure 4b), whereas the $\Delta R/R_o$ value of the carbon nanotube (CNT) sponge was larger than 60%. The excellent flexibility of the AgNFs and the strong connection of junctions were critical to form this robust macroscopically continuous 3D silver sponge. A small piece of the sponge was observed in SEM. The silver fibers were interwoven and well distributed, as shown in Figure 4c. The silver sponge contained numerous holes, as shown in Figure 4d; the diameter of the nanofibers was around 400 nm. Figure S9 shows a 40 cm^3, 100 mg silver sponge (2.5 mg/cm^3 sponge). Ultralight 3D materials are desirable in many applications, such

DOI: 10.1021/acs.nanolett.6b02654
Nano Lett. 2016, 16, 5846−5851

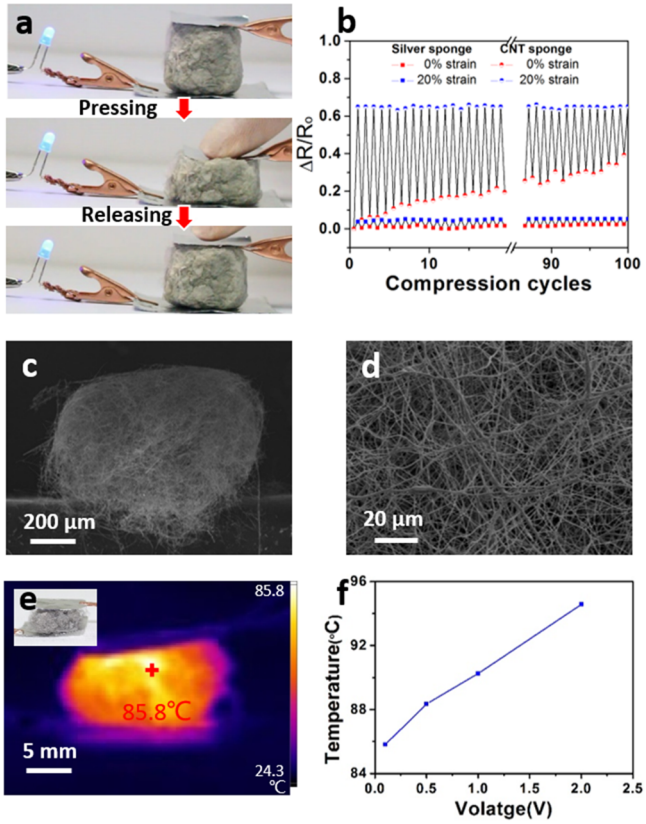

Figure 4. Morphology and application of silver sponge. (a) Photographs of the "silver sponge" pressed by a finger and recovered after releasing pressure. (b) Resistance change in pressing measurement compared with the CNT sponge. SEM images of (c) the silver sponge and (d) its internal structure. (e) Infrared thermal image showing temperature distribution over the AgNF sponge during operation. (f) Plot of the AgNF sponge temperature at steady state versus voltage.

as battery electrodes, catalyst supports, shock energy damping, and heating devices.

A Joule heating device by flexible AgNF sponge has been shown in Figure 4e. AgNF network has various applications such as in outdoor panel displays, window defrosters, liquid crystal display panels for harsh environment.[8,33] The structure and principle of AgNF conductor are simple, but its high-performance operation with a low voltage and rapid response can be achieved only with a superior felxible electrode. In our device, the DC voltage was supplied to the AgNF sponge through silver paste contacts at the edge, and the temperature was monitored using an infrared thermal imaging camera. Figure 4e is a representative steady-state thermal image of an AgNF sponge with a resistance of 100 Ω and which is powered by an applied voltage of 0.1 V. Regardless of the input voltages, the steady-state temperature of the AgNF sponge was reached within 3 s, demonstrating the rapid response of the device. The center temperature of the AgNF sponge reached 85 °C under 0.1 V, confirming its operation at low input voltages. Control of the AgNF sponge temperature was achieved by adjusting the supplied voltage as shown in Figure 4f. Unless AgNF sponge could be fabricated as a Joule heater, AgNF network heater is also feasible. Figure S12 is a representative steady-state thermal image of a AgNF network with a sheet resistance of 10 Ω sq^{-1} and which is powered by an applied voltage of 0.5 and 1 V and the temperature is above 200 °C.

In conclusion, we fabricated highly flexible 2D and 3D conductors based on AgNFs via a modified blow spinning method, which is inexpensive and quick. The conductivity and mechanical performance of the AgNF network were better than most flexible conductive electrodes reported and could be demonstrated in the application of flexible circuits. The 3D silver sponge entangled by silver fibers sustained mechanical damage and retained conductivity. Both 2D and 3D conductors were produced via large-scale fabrication. The remarkable performance of AgNFs may be attributed to the following main factors. First, the silver grains in the fiber attached to one another firmly, and this arrangement benefitted electron transportation in single AgNF. Second, the AgNF was ultralong, and the conducting network was a combination of microscale and nanoscale fibers. This structure is ideal for silver fiber electrodes. Third, traces of carbon in the AgNF acted on lubrication and improved the flexibility of the AgNF network.

■ ASSOCIATED CONTENT

Supporting Information

The Supporting Information is available free of charge on the ACS Publications website at DOI: 10.1021/acs.nanolett.6b02654.

Details of sample preparation, data acquisition, and the data analysis (PDF)

Pressing measurement of silver sponge (AVI)

Crushing experiment and bending test of silver nanowire networks (AVI)

■ AUTHOR INFORMATION

Corresponding Author

*E-mail: huiwu@tsinghua.edu.cn.

Author Contributions

Y. H. and X.B. contribute to this work equally.

Notes

The authors declare no competing financial interest.

■ ACKNOWLEDGMENTS

This study was supported by the National Basic Research of China (Grants 2015CB932500 and 2013CB632702) and the NSF of China (Grants 51522207 and 51302141).

■ REFERENCES

(1) Russo, A.; Ahn, B. Y.; Adams, J. J.; Duoss, E. B.; Bernhard, J. T.; Lewis, J. A. *Adv. Mater.* **2011**, *23*, 3426−3430.

(2) Ma, R.; Kwon, S.; Zheng, Q.; Kwon, H. Y.; Kim, J. I.; Choi, H. R.; Baik, S. *Adv. Mater.* **2012**, *24*, 3344−3349.

(3) Lipomi, D. J.; Vosgueritchian, M.; Tee, B. C. K.; Hellstrom, S. L.; Lee, J. A.; Fox, C. H.; Bao, Z. *Nat. Nanotechnol.* **2011**, *6*, 788−792.

(4) Ye, S.; Rathmell, A. R.; Chen, Z.; Stewart, I. E.; Wiley, B. J. *Adv. Mater.* **2014**, *26*, 6670−6687.

(5) Layani, M.; Kamyshny, A.; Magdassi, S. *Nanoscale* **2014**, *6*, 5581−5591.

(6) Kumar, A.; Zhou, C. *ACS Nano* **2010**, *4*, 11−14.

(7) Sun, Y.; Xia, Y. *Nature* **1991**, *353*, 737.

(8) Khan, A.; Lee, S.; Jang, T.; Xiong, Z.; Zhang, C.; Tang, J.; Guo, L. J.; Li, W. D. *Small* **2016**, *12*, 3021−3030.

(9) Ellmer, K. *Nat. Photonics* **2012**, *6*, 809−817.

(10) Hsu, P. C.; Wang, S.; Wu, H.; Narasimhan, V. K.; Kong, D.; Lee, H. R.; Cui, Y. *Nat. Commun.* **2013**, *4*, 4.

(11) Lee, J. Y.; Connor, S. T.; Cui, Y.; Peumans, P. *Nano Lett.* **2008**, *8*, 689−692.

DOI: 10.1021/acs.nanolett.6b02654
Nano Lett. 2016, 16, 5846−5851

(12) Deng, B.; Hsu, P. C.; Chen, G.; Chandrashekar, B. N.; Liao, L.; Ayitimuda, Z.; Wu, J.; Guo, Y.; Lin, L.; Zhou, Y.; Aisijiang, M.; Xie, Q.; Cui, Y.; Liu, Z.; Peng, H. *Nano Lett.* **2015**, *15*, 4206−4213.
(13) Garnett, E. C.; Cai, W.; Cha, J. J.; Mahmood, F.; Connor, S. T.; Christoforo, M. G.; Cui, Y.; McGehee, M. D.; Brongersma, M. L. *Nat. Mater.* **2012**, *11*, 241−249.
(14) Lee, J.; Lee, P.; Lee, H.; Lee, D.; Lee, S. S.; Ko, S. H. *Nanoscale* **2012**, *4*, 6408−6414.
(15) Lu, H.; Zhang, D.; Ren, X.; Liu, J.; Choy, W. C. *ACS Nano* **2014**, *8*, 10980−10987.
(16) Triambulo, R. E.; Cheong, H. G.; Park, J. W. *Org. Electron.* **2014**, *15*, 2685−2695.
(17) He, X.; He, R.; Liu, A.; Chen, X.; Zhao, Z.; Feng, S.; Chen, N.; Zhang, M. *J. Mater. Chem. C* **2014**, *2*, 9737−9745.
(18) Yu, Z.; Zhang, Q.; Li, L.; Chen, Q.; Niu, X.; Liu, J.; Pei, Q. *Adv. Mater.* **2011**, *23*, 664−668.
(19) Han, B.; Huang, Y.; Li, R.; Peng, Q.; Luo, J.; Pei, K.; Herczynski, A.; Kempa, K.; Ren, Z.; Gao, J. *Nat. Commun.* **2014**, *5*, 5674.
(20) Yu, Y.; Zeng, J.; Chen, C.; Zhuang, X.; Guo, R.; Liu, Z.; Zhou, X.; Yang, Y.; Zheng, Z. *Adv. Mater.* **2014**, *26*, 810−815.
(21) Yeo, W. H.; Kim, Y. S.; Lee, J.; Ameen, A.; Shi, L.; Li, M.; Wang, S.; Ma, R.; Jin, S. H.; Kang, Z.; Huang, Y.; Rogers, J. A. *Adv. Mater.* **2013**, *25*, 2773−2778.
(22) Webb, R. C.; Bonifas, A. P.; Behnaz, A.; Zhang, Y.; Yu, K. J.; Cheng, H.; Shi, M.; Bian, Z.; Liu, Z.; Kim, Y. S.; Yeo, W. H.; Park, J. S.; Song, J.; Li, Y.; Huang, Y.; Gorbach, A. M.; Rogers, J. A. *Nat. Mater.* **2013**, *12*, 938−944.
(23) Yu, Y.; Yan, C.; Zheng, Z. *Adv. Mater.* **2014**, *26*, 5508−5516.
(24) Fantino, E.; Chiappone, A.; Roppolo, I.; Manfredi, D.; Bongiovanni, R.; Pirri, C. F.; Calignano, F. *Adv. Mater.* **2016**, *28* (19), 3711−3711.
(25) Kim, D. H.; Xiao, J.; Song, J.; Huang, Y.; Rogers, J. A. *Adv. Mater.* **2010**, *22*, 2108−2124.
(26) Schaedler, T. A.; Jacobsen, A. J.; Torrents, A.; Sorensen, A. E.; Lian, J.; Greer, J. R.; Valdevit, L.; Carter, W. B. *Science* **2011**, *334*, 962−965.
(27) Wu, C.; Huang, X.; Wang, G.; Lv, L.; Chen, G.; Li, G.; Jiang, P. *Adv. Funct. Mater.* **2013**, *23*, 506−513.
(28) Shan, C.; Zhao, W.; Lu, X. L.; O'Brien, D. J.; Li, Y.; Cao, Z.; Elias, A. L.; Cruz-Silva, R.; Terrones, M.; Wei, B.; Suhr, J. *Nano Lett.* **2013**, *13*, 5514−5520.
(29) Sun, Y. *Nanoscale* **2010**, *2*, 1626−1642.
(30) Dzenis, Y. A. *Science* **2004**, *304*, 1917−1919.
(31) Li, D.; Xia, Y. *Adv. Mater.* **2004**, *16*, 1151−1170.
(32) Medeiros, E. S.; Glenn, G. M.; Klamczynski, A. P.; Orts, W. J.; Mattoso, L H C. *J. Appl. Polym. Sci.* **2009**, *113*, 2322−2330.
(33) An, B. W.; Gwak, E. J.; Kim, K.; Kim, Y. C.; Jang, J.; Kim, J. Y.; Park, J. U. *Nano Lett.* **2016**, *16* (1), 471−478.
(34) Wu, H.; Kong, D.; Ruan, Z.; Hsu, P. C.; Wang, S.; Yu, Z.; Carney, T. J.; Hu, L.; Fan, S.; Cui, Y. *Nat. Nanotechnol.* **2013**, *8*, 421−425.
(35) Leem, D. S.; Edwards, A.; Faist, M.; Nelson, J.; Bradley, D. D.; de Mello, J. C. *Adv. Mater.* **2011**, *23*, 4371−4375.
(36) Bae, S.; Kim, H.; Lee, Y.; Xu, X.; Park, J. S.; Zheng, Y.; Kim, Y. J. *Nat. Nanotechnol.* **2010**, *5*, 574−578.
(37) Hecht, D. S.; Hu, L.; Irvin, G. *Adv. Mater.* **2011**, *23*, 1482−1513.

DOI: 10.1021/acs.nanolett.6b02654
Nano Lett. 2016, 16, 5846−5851